Electronic Supplementary Material (ESI) for Journal of Materials Chemistry A.
This journal is © The Royal Society of Chemistry 2018

Supplementary Information

For

Self-templating synthesis of silicon nanorods from nature sepiolite for high-performance lithium-ion battery anodes

Qingze Chen[a, b], Runliang Zhu[a] *, Shaohong Liu[c], Dingcai Wu[c], Haoyang Fu[a, b], Jianxi Zhu[a], Hongping He[a]

[a] *CAS Key Laboratory of Mineralogy and Metallogeny, Guangdong Provincial Key Laboratory of Mineral Physics and Material, Guangzhou Institute of Geochemistry, Chinese Academy of Sciences, Guangzhou 510640, China*

[b] *University of Chinese Academy of Sciences, Beijing 100049, China*

[c] *Materials Science Institute, PCFM Lab and GDHPRC Lab, School of Chemistry, Sun Yat-sen University, Guangzhou, P. R. China*

* Corresponding author

Prof. Runliang Zhu, E-mail: zhurl@gig.ac.cn

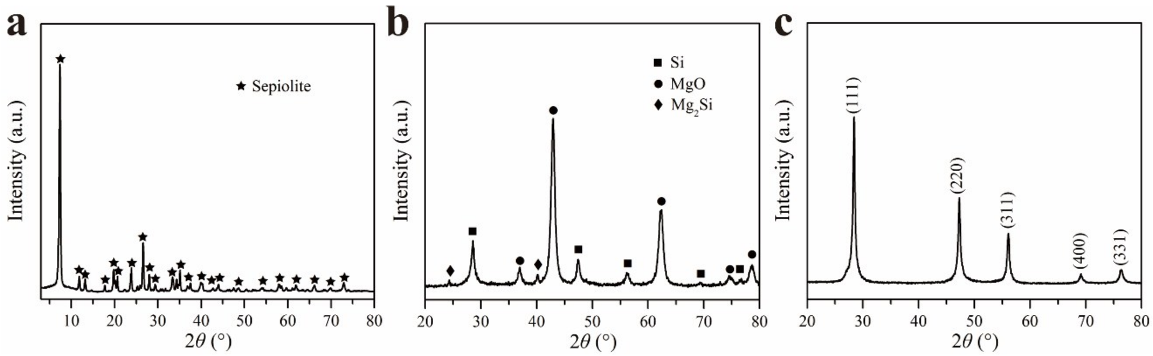

Fig. S1 XRD patterns of sepiolite (a), the intermediates after magnesiothermic reduction reaction (b), and finally silicon products SNRs (c).

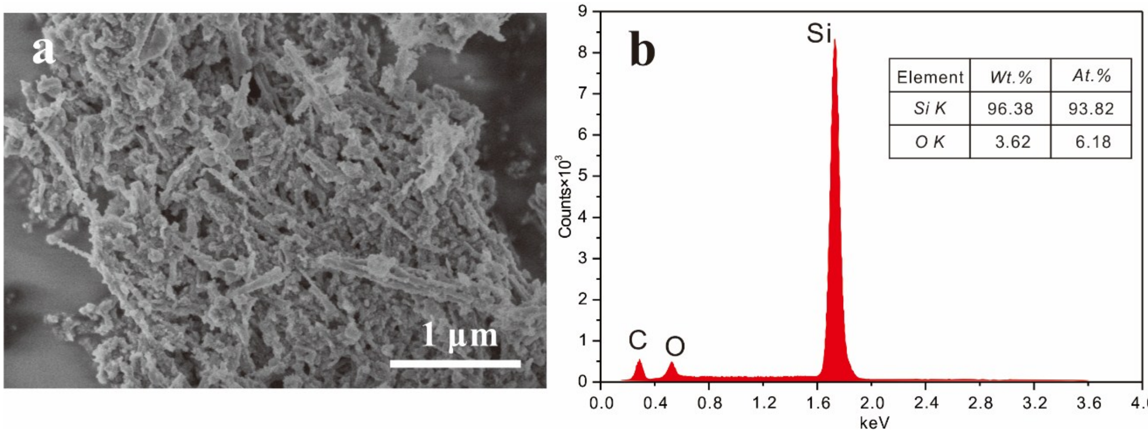

Fig. S2 SEM image (a) and EDS spectrum (b) of SNRs.

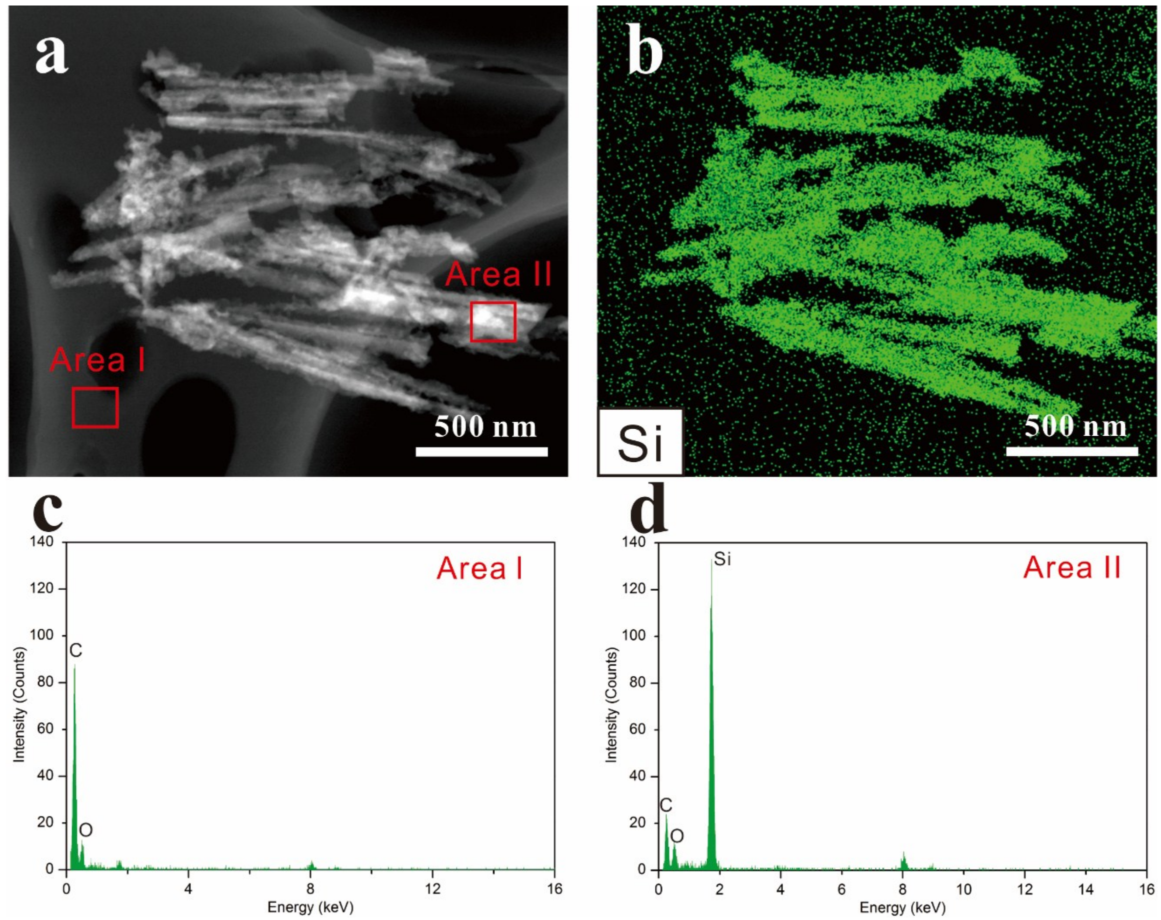

Fig. S3 The dark-field TEM image of SNRs (a) and the corresponding EDS mapping of elemental Si (b). The EDS spectra of area I on the background (c) and area II on the SNRs (d).

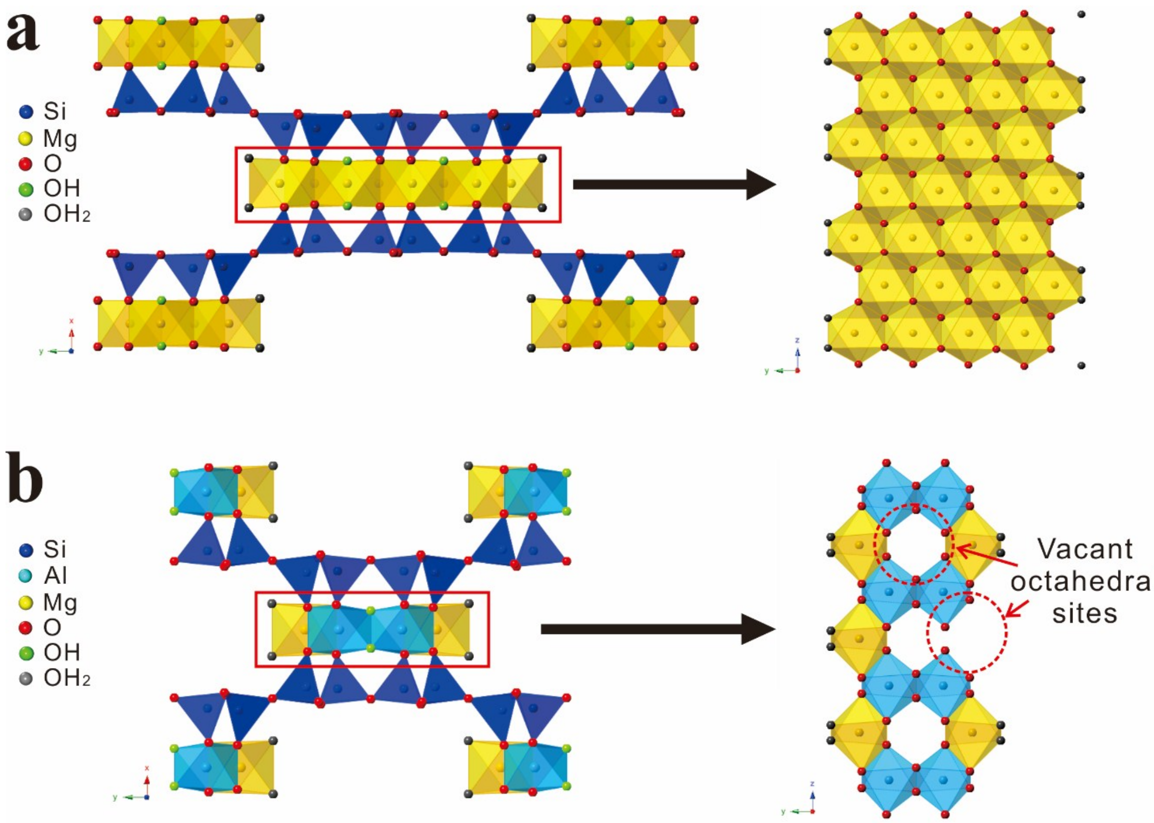

Fig. S4 Crystal structrues (lateral views) and the corresponding octahedral sheets (top views). (a) Sepiolite, and (b) palygorskite.

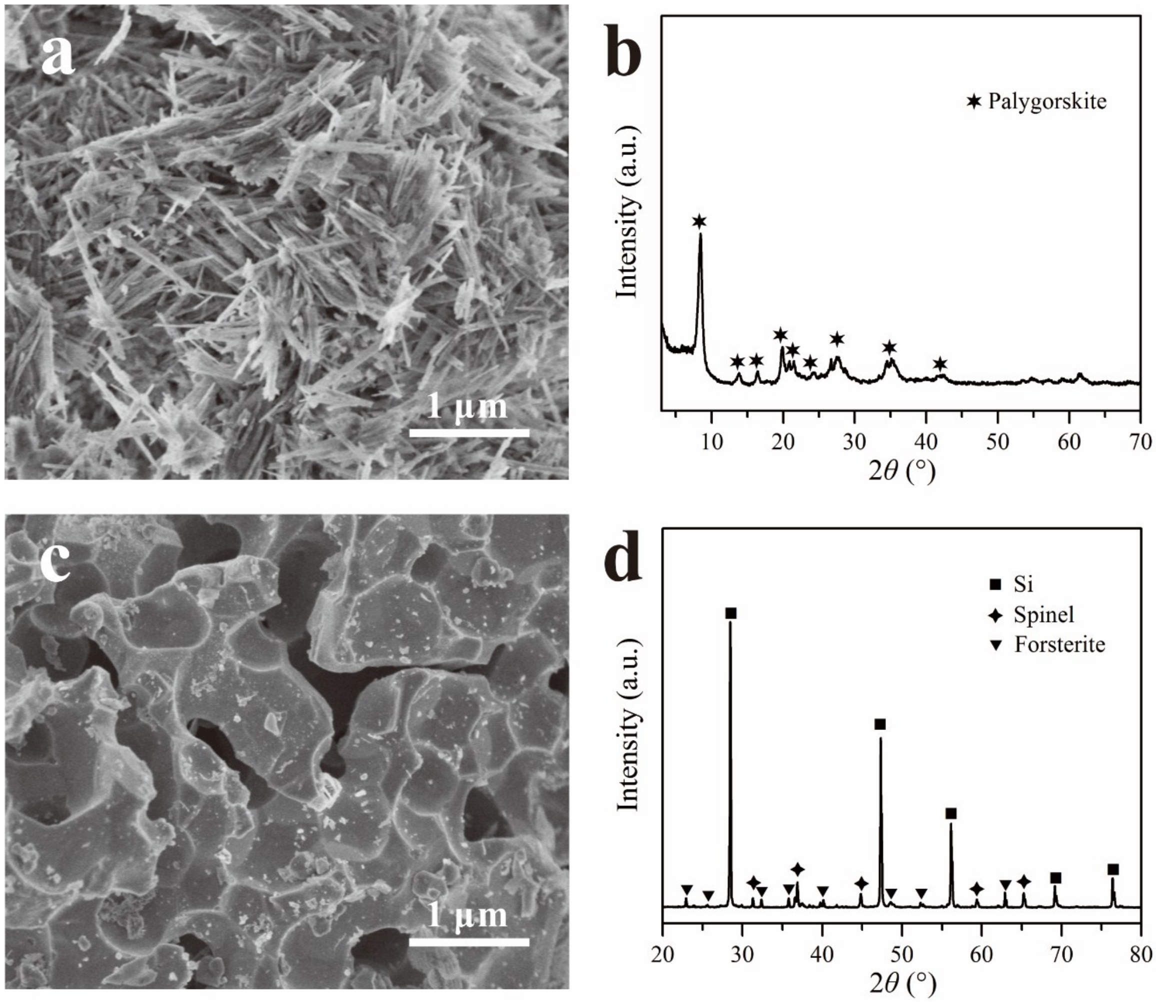

Fig. S5 SEM image (a) and XRD pattern (b) of palygorskite. SEM image (c) and XRD pattern (d) of the final silicon products from palygorskite under the same preparation conditions as sepiolite.

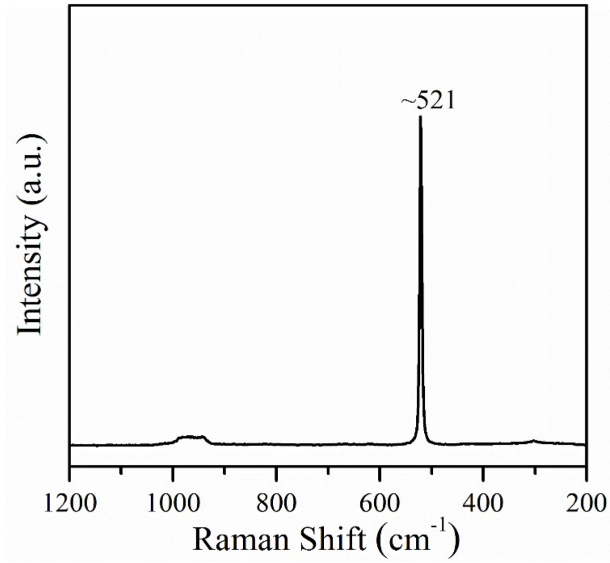

Fig. S6 Raman spectrum of monocrystalline Si.

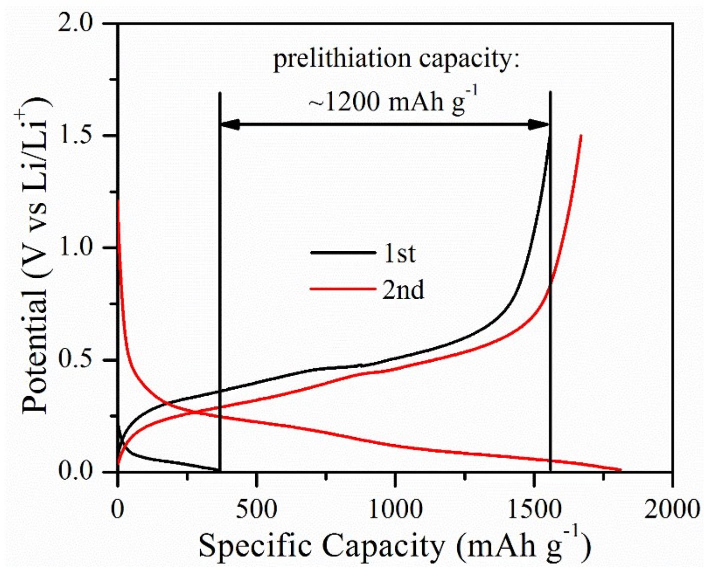

Fig. S7 First cycle discharge/charge voltage profiles of prelithiated electrode for 20 min at a current density of 0.2 A g^{-1}.

Typically, a SNR electrode was in direct contact with a lithium metal foil with electrolyte injected between them. External pressure was applied on them. After prelithiation for 20 min, the SNR electrode was peeled off from the lithium metal and washed with acetonitrile. Finally, the prelithiated SNR half-cell was assembled.

As shown by the first cycle discharge/charge voltage profiles, the prelithiated SNR electrode didn't have enough time to form full lithium alloy, and thus showed a plateau corresponding to alloying of Si and Li. Right after the first cycle, the prelithiated SNR electrode exhibited remarkably enhanced CE of 92%, compared to that of raw SNR (~61%). The result clearly indicated that the insufficient initial CE of SNR electrodes could be overcome by the simple prelithiation.

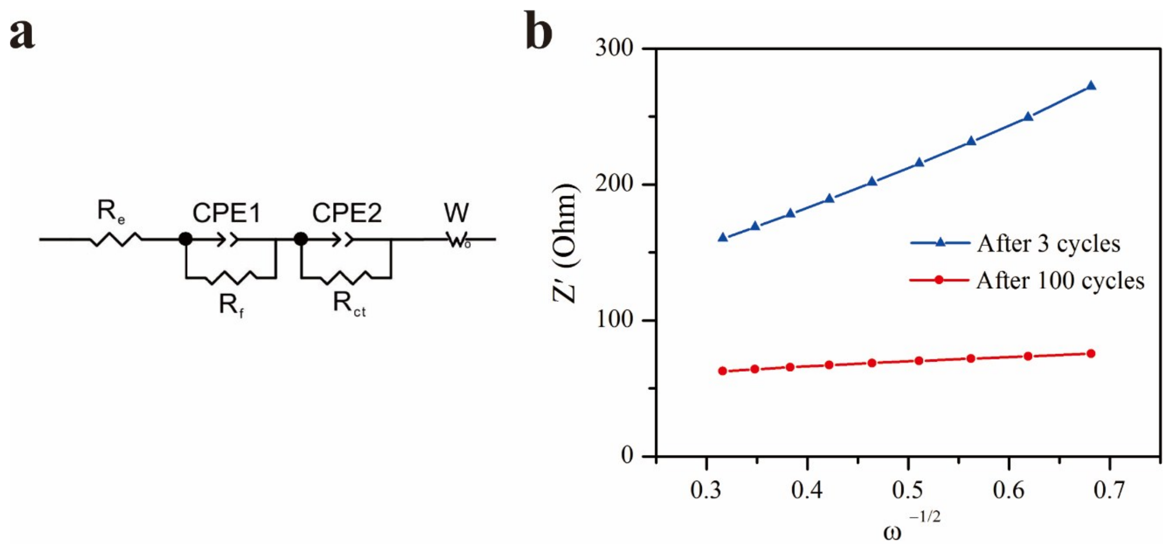

Fig. S8 (a) Equivalent circuit of the electrochemical impedance spectroscopy spectra (R_e: the electrolyte resistance; R_f: the ohmic resistance in the interface of the SEI film; R_{ct}: the charge transfer resistance at the electrode-electrolyte interface; W: the Warburg impedance term for the solid state diffusion of lithium ions; CPE1 and CPE2: the two resistors with constant phase elements)[1]. (b) The relationship between Z' and $\omega^{-1/2}$ in the low frequency region.

The fitted data based on the equivalent circuit showed that the electrode after 3 and 100 cycles possessed the R_{ct} values of 108 and 72 Ω, respectively, which indicate that the electrode showed the faster charge transfer kinetics after 100 cycles. Moreover, the relationship between Z' and $\omega^{-1/2}$ in the low frequency region were plotted. The slope of the curve represented the Warburg coefficient (σ_w), which was inversely proportional to the diffusivity of lithium ions.[2] The calculated σ_w values for the electrode after 3 and 100 cycles were 304 and 35 Ω $s^{-1/2}$, respectively. The smaller σ_w of the electrode after 100 cycles suggested the better diffusion of lithium ions than that after 3 cycles.

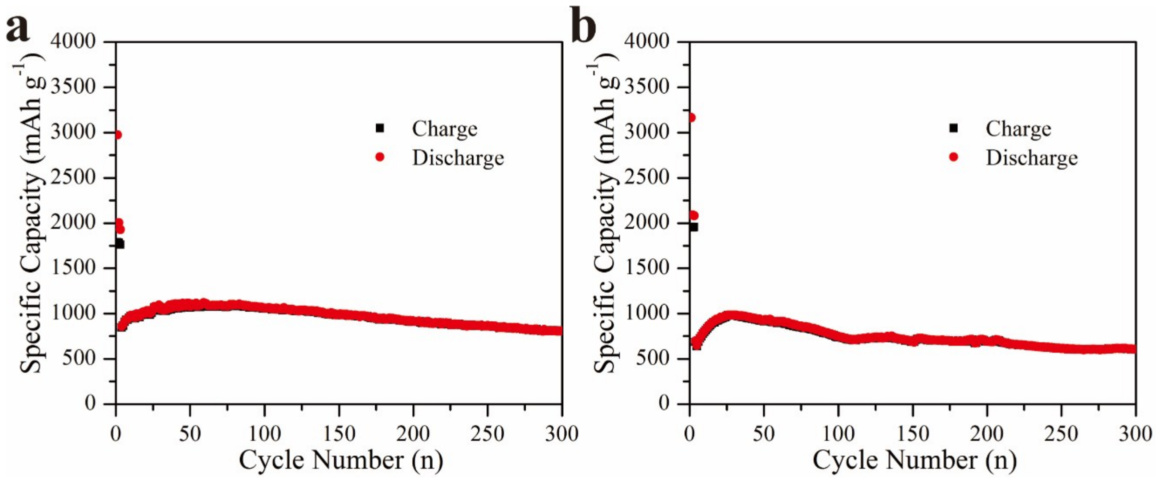

Fig. S9 (a) The cycling performance of the SNR electrode prepared with a ratio of active material, binder, and conductive agent (6: 2: 2), corresponding to an active mass loading of ~1.1 mg cm^{-2}. (b) and the cycling performance of the SNR electrode prepared with with a ratio of active material, binder, and conductive agent (7: 1.5: 1.5), corresponding to an active mass loading of ~0.8 mg cm^{-2}. All the measurements were carried out at current densities of 0.2 A g^{-1} for the initial three cycles and 5.0 A g^{-1} for the remaining cycles.

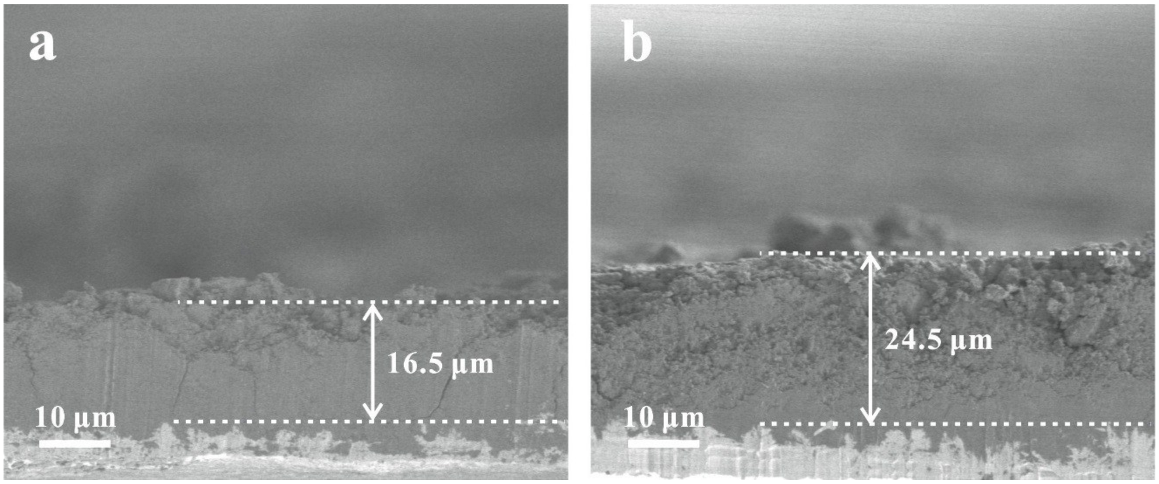

Fig. S10 Cross-sectional SEM images showing the volume expansion of the SNR electrodes before electrochemical test (a) and after 100 cycles at 1.0 A g^{-1} (c).

Table S1 Summary for electrochemical performances of 1D nanostructrued Si anodes synthesized by various methods in this work and in previous studies.

Si-based anodes	**Rate performance**	**Capacity retention**	**Loading mass (mg/cm^2)**	**Volume expansion**	**Methods**	**Ref.**
Si nanorods	478 mAh g^{-1} at 10 A g^{-1}	816 mAh g^{-1} at 5.0 A g^{-1} after 500 cycles, retention ~98%	~0.7	~50%	Self-templating involved in magnesiothermic reduction	This work
Carbon coated Si nanorods	420 mAh g^{-1} at 4.0 A g^{-1}	~700 mAh g^{-1} at 1.0 A g^{-1} after 1000 cycles, retention ~80%	0.9	Retained	Acid etching rapidly solidified eutectic Al-Si ingot	[3]
Mesoporous Si nanorod	664 mAh g^{-1} at 2.0 A g^{-1}	~1038 mAh g^{-1} at 0.2 A g^{-1} after 170 cycles, retention ~70%	0.9	-	MWCNTs as a template via a magnesiothermic reduction	[4]
Si nanowires	>2100 mAh g^{-1} at 4.2 A g^{-1}	~3500 mAh g^{-1} at 0.84 A g^{-1} after 20 cycles, retention ~90%	~0.5	~400%	Vapour-liquid-solid or vapour-solid template-free growth methods	[5]
Si nanowires	>900 mAh g^{-1} at 42 A g^{-1}	~1030 mAh g^{-1} at 2.0 A g^{-1} after 1000 cycles, retention ~33%	0.03~0.04	Aggregated	Vapour-liquid-solid growth based on anodized aluminum oxide templates	[6]
Si nanotubes	~600 mAh g^{-1} at 21 A g^{-1}	1287 mAh g^{-1} at 0.84 A g^{-1} after 200 cycles, retention ~40%	~0.13	-	ZnO templates-assisted chemical vapor deposition	[7]
Carbon coated Si nanotubes	1900 mAh g^{-1} at 0.4 A g^{-1}	~900 mAh g^{-1} at 0.4 A g^{-1} after 90 cycles, retention ~50%	-	-	Electrospinning followed by magnesiothermic reduction	[8]
Si nanofibers	>500 mAh g^{-1} at 80 A g^{-1}	~1363 mAh g^{-1} at 2.0 A g^{-1} after 300 cycles, retention ~70%	0.4~0.6	-	Electrospinning followed by magnesiothermic reduction	[9]
Si nanowires	~521 mAh g^{-1} at 4.2 A g^{-1}	~714 mAh g^{-1} at 2.1 A g^{-1} after 500 cycles, retention ~25%	1.1	-	Electrochemical reduction of $CaSiO_3$ in molten salts	[10]
Carbon coated Si nanowires	>1000 mAh g^{-1} at 0.3 A g^{-1}	~1326 mAh g^{-1} at 0.15 A g^{-1} after 40 cycles, retention ~40%	-	-	Metal-catalyzed electroless etching of silicon wafers	[11]
Polypyrrole coated Si nanowires	~150 mAh g^{-1} at 3 A g^{-1}	~611 mAh g^{-1} at 0.3 A g^{-1} after 200 cycles, retention ~21%	-	Partially remained	Sol−gel nanocoating technique followed by magnesiothermic reduction	[12]

References

1. J. Liang, X. N. Li, Z. G. Hou, W. Q. Zhang, Y. C. Zhu and Y. T. Qian, *ACS Nano*, 2016, **10**, 2295-2304.
2. W. Duan, Z. Zhu, H. Li, Z. Hu, K. Zhang, F. Cheng and J. Chen, *J. Mater. Chem. A*, 2014, **2**, 8668-8675.
3. J. Wang, X. Meng, X. Fan, W. Zhang, H. Zhang and C. Wang, *ACS Nano*, 2015, **9**, 6576-6586.
4. Y. Zhou, X. Jiang, L. Chen, J. Yue, H. Xu, J. Yang and Y. Qian, *Electrochim. Acta* 2014, **127**, 252-258.
5. C. K. Chan, H. Peng, G. Liu, K. McIlwrath, X. F. Zhang, R. A. Huggins and Y. Cui, *Nat. Nanotechnol.* , 2008, **3**, 31-35.
6. J.-H. Cho and S. T. Picraux, *Nano Lett.* , 2013, **13**, 5740-5747.
7. E. M. Lotfabad, P. Kalisvaart, A. Kohandehghan, K. Cui, M. Kupsta, B. Farbod and D. Mitlin, *J. Mater. Chem. A*, 2014, **2**, 2504-2516.
8. J.-K. Yoo, J. Kim, Y. S. Jung and K. Kang, *Adv. Mater.* , 2012, **24**, 5452-5456.
9. D. J. Lee, H. Lee, M.-H. Ryou, G.-B. Han, J.-N. Lee, J. Song, J. Choi, K. Y. Cho, Y. M. Lee and J.-K. Park, *ACS Appl. Mater. Inter.*, 2013, **5**, 12005-12010.
10. Y. F. Dong, T. Slade, M. J. Stolt, L. S. Li, S. N. Girard, L. Q. Mai and S. Jin, *Angew. Chem., Int. Ed.*, 2017, **56**, 14453-14457.
11. R. Huang, X. Fan, W. Shen and J. Zhu, *Appl. Phys. Lett.* , 2009, **95**.
12. J. Li and J. Huang, *Chem. Commun.* , 2015, **51**, 14590-14593.